Middle East Research Journal of Engineering and Technology
ISSN: 2789-7737 (Print) ISSN: 2958-2059 (Online)
Frequency: Bi-Monthly
DOI: 10.36348/merjet.2024.v04i02.001

KUWAIT SCHOLARS PUBLISHER
Website: http://www.kspublisher.com/
Email: office@kspublisher.com

Utilizing Electrochemical Techniques for Assessing the Probability of Concrete Resistivity and Corrosion Potential in Reinforced Concrete Structures

Bright Akoba[1*], Uche Christian Ajah[2], Charles Kennedy[3]
[1]School of Engineering, Department of Electrical/Electronic Engineering, Kenule Beeson Saro-Wiwa Polytechnic, Bori, Rivers State, Nigeria
[2]Department of Civil Engineering Technology, Akanulbiam Federal Polytecgnic, Unwana, Afikpo, Ebony State, Nigeria
[3]School of Engineering, Department of Civil Engineering, Kenule Beeson Saro-Wiwa Polytechnic, Bori, Rivers State, Nigeria

Abstract: Corrosion of reinforcing steel is a major durability issue for reinforced concrete structures exposed to aggressive environments. Early assessment of corrosion probability is important for effective maintenance planning. This study investigates the application of non-destructive electrochemical methods like concrete resistivity and half-cell potential measurement, along with integrated assessment and advanced techniques, for evaluating corrosion risk in reinforced concrete. Concrete specimens with and without Albizia amara resin coating were subjected to accelerated corrosion testing. Concrete resistivity and half-cell potential values showed an inverse correlation, with lower resistivity indicating higher corrosion risk. Resistivity and potential results for the coated samples exhibited intermediate values compared to the control and corroded samples, demonstrating the resin's partial passivating effects. Rebar diameter measurements before and after exposure confirmed corrosion led to reductions in diameter and cross-sectional area, which coating mitigated. Statistical analysis validated the significant impacts of original bar diameter and corrosion level on subsequent geometry changes. Mechanical testing of reinforcing steel bars found the control samples had the highest strength and ductility, while the coated bars exhibited properties closer to the controls than the corroded bars. The protective capabilities of the bio-based Albizia amara resin coating were validated through multipoint monitoring of material durability parameters. Overall, results demonstrated the effectiveness of integrated electrochemical testing with non-destructive techniques for comprehensive condition assessment and corrosion risk evaluation in reinforced concrete structures.

Keywords: Reinforced Concrete, Corrosion, Electrochemical Techniques, Resistivity, Half-Cell Potential, Corrosion Inhibitor, Coating, Durability.

Research Paper

***Corresponding Author:**
Bright Akoba
School of Engineering, Department of Electrical/Electronic Engineering, Kenule Beeson Saro-Wiwa Polytechnic, Bori, Rivers State, Nigeria

How to cite this paper:
Bright Akoba *et al* (2024). Utilizing Electrochemical Techniques for Assessing the Probability of Concrete Resistivity and Corrosion Potential in Reinforced Concrete Structures. *Middle East Res J. Eng. Technol*, *4*(2): 21-38.

Article History:
| Submit: 19.05.2024 |
| Accepted: 20.06.2024 |
| Published: 27.06.2024 |

1. INTRODUCTION

Reinforced concrete is widely used in construction due to its high compressive strength, flexibility to mold into various structural forms, and relatively low cost (Wang & Monteiro, 1996). However, corrosion of the embedded steel reinforcement is a major durability issue, especially when exposed to aggressive environments containing chlorides from deicing salts, marine exposure, or other sources (Gaidis & Rosenberg, 1987). Corrosion leads to cracking, delamination and spalling of the concrete cover, which further accelerates corrosion by exposing more steel surface area. As the rebar cross-section is reduced by corrosion penetration, both the strength and service life of reinforced concrete structures are compromised (Hansson *et al.*, 1998). Therefore, early evaluation of the risk and probability of corrosion is critical for effective maintenance and repair planning.

Concrete resistivity measurement using Wenner probe method and half-cell potential mapping using a reference electrode are commonly used non-destructive electrochemical techniques for assessing the likelihood of reinforcement corrosion in concrete structures (Justnes, 2003). While resistivity provides qualitative information about the corrosivity of the concrete bulk matrix, half-cell potential indicates quantitative data regarding the actual corrosion state of the embedded rebar (Ormellese *et al.*, 2006).

Resistivity indicates the ability of concrete to conduct electricity, which depends on its pore structure, moisture content, ionic concentration and other physico-chemical factors (Soylev & Richardson, 2008). Concrete with low resistivity allows easier mobility of chloride and other ions, indicating higher corrosion risk for the embedded steel (Macmammah *et al.*, 2021). The Wenner four-probe method is widely accepted for measuring

concrete resistivity. In this technique, four equally spaced probes are placed on the concrete surface. An AC current is passed between the outer probes and the potential drop is measured between the inner probes (Charles *et al*., 2018). The bulk resistivity is then calculated using the current, potential and probe spacing.

Typical concrete resistivity values below100 Ω-m indicate high ionic mobility and corrosion risk for steel compared to values above 200 Ω-m which signify negligible to low risk (Charles *et al*., 2018). However, resin-rich and saturated areas of concrete may show lower resistivity despite low chloride content. So, the bulk resistivity results should be interpreted in conjunction with chloride analysis and other parameters (Macmammah *et al*., 2021).

Factors Influencing Concrete Resistivity

Resistivity of concrete is influenced by multiple factors such as moisture content, temperature, chloride concentration, pore solution chemistry, curing duration and quality of construction (Achieme *et al*., 2021). Higher water-cement ratio increases porosity and ion mobility, lowering resistivity. Proper moist curing densifies the microstructure thereby increasing resistivity and durability. Temperature variations cause seasonal changes in resistivity due to effects on pore fluid chemistry. Resistivity is also substantially lowered by moisture and chloride ingress (Al-Moudi *et al*., 2003). Therefore, field resistivity results need corrections for variability in moisture content and temperature.

The corrosion tendency of embedded steel rebar can be assessed by measuring the potential difference between the steel and a standard reference electrode placed on the concrete surface (Dalo-Abu *et al*., 2012). The copper-copper sulphate half-cell is most commonly used as reference electrode for this purpose. Corrosion probability is determined as per ASTM C876 specifications – half-cell potential more negative than -350 mV has >90% corrosion risk. However, the range between -200 to -350 mV indicates uncertain probability requiring further evaluation (Umoren *et al*., 2008).

The half-cell potential measurement requires sufficient wetting of the concrete surface. A high impedance voltmeter minimizing current flow is used for accurate potential measurement. The reference electrode is moved grid-wise on the concrete and the potentials mapped for identifying anodic and cathodic areas. Probable corroding locations are identified where potential is more negative than surrounding areas (Umoren, 2009).

The measured half-cell potential is influenced by multiple factors like chloride concentration, carbonation depth, concrete resistivity, rebar depth, oxygen transport, and macrocell formation (Charles *et al*., 2018). Penetration of chlorides through the concrete cover breaks down the passive film on steel and shifts the potential to more negative values (Jano *et al*., 2012). Carbonation reduces the pore solution pH, also lowering the potential. Areas of low resistivity and shallow rebar depth exhibit more negative potentials. Poor oxygen availability limits cathodic sites and makes the potential more positive (Charles *et al*., 2018).

While resistivity provides qualitative information about the corrosivity of concrete bulk matrix, half-cell potential mapping gives quantitative data for probability of corrosion at the rebar location (Gowers & Millard, 1999b). Integrated assessment using both these techniques provides a comprehensive evaluation of contributing factors for appropriate maintenance decisions (Layssi *et al*., 2015). Locations with low resistivity and potential more negative than -350 mV indicate high risk of active corrosion. However, discrepancies in resistivity and potential data need to be analyzed in conjunction with cover depth, saturation and chloride content for reliably assessing corrosion risk (Luo *et al*., 2018).

Advanced Electrochemical Techniques

In addition to Wenner probe and half-cell potential measurements, advanced electrochemical techniques like linear polarization resistance, electrochemical impedance spectroscopy and cyclic potentiodynamic polarization can also be utilized for in-depth analysis of steel-concrete interface (Joiret *et al*., 2002). Though these techniques require extensive instrumentation and specialized data analysis methods, very useful information is obtained regarding corrosion kinetics, mechanism and passivation at the rebar surface to support maintenance strategies (Poursaee & Hansson, 2007).

2.1 MATERIALS AND METHODS

2.1.1 Aggregates

Fine and coarse aggregates were purchased and verified to meet the requirements of BS 8821.

2.1.2 Cement

Lime cement grade 42.5 was utilized in all concrete mixtures and verified to meet the guidelines of BS EN 196-6.

2.1.3 Water

Water samples were collected from the laboratory and verified to conform to the requirements of BS 3148.

2.1.4 Structural Reinforcement

Structural reinforcement was procured directly from the market and met BS4449: 2005 + A3 regulations.

2.1.5 Corrosion Inhibitors (Plastics / Waste) Albizia Amara

Residue from the harvesting of a tree trunk from Auwaru Village in Akko Gombe State Local Government, Nigeria was used as an anti-corrosive

material against corrosive attack on reinforced concrete structures in coastal areas with high salt concentration and extreme conditions.

2.2 Experimental Procedure

2.2.1 Experimental Method

This research explored the effect of applying the resin extracted from the stem of the Albizia amara plant as a corrosion inhibitor on reinforced concrete structures exposed to corrosive environments with high salt concentrations. To test the corrosion resistance of concrete, an experimental method was developed to accelerate the corrosion process and maximize the corrosion resistance of the material.

2.2.2 Preparation of Samples for Reinforcement of Resin / Exudate Coating

Model concrete slabs with dimensions 100 mm × 500 mm × 500 mm (thickness, width, and length) were cast using a metal mold and hand-mixed with a standard concrete ratio of 1.2.4 and a water-cement ratio of 0.65. The reinforced concrete slabs were then compacted and reinforced with 10 steel bars of 12mm diameter, set at 100mm c / c (top and bottom), and cured at standard room temperature for 28 days. The hardened slabs were subsequently submerged in a 5% aqueous sodium chloride (NaCl) solution and accelerated for 360 days under accelerated conditions induced by corrosion and tested periodically for 90 days, 180 days, 270 days, and 360 days. Both uncoated and coated samples were tested for performance.

2.3 Accelerated Corrosion Test

Accelerated corrosion testing is an effective technique for testing the corrosion of steel in concrete and evaluating the protective layer of the concrete against the reinforcement. For the appropriate selection of materials and protection systems, accelerated corrosion tests were performed to obtain quantitative and qualitative corrosion information.

2.4 Corrosion Current Measurement (Half-Cell Potential Measurement)

The classification of corrosion of steel bars is shown in Table 2.1. If the results of the potential measurement show a high possibility of corrosion, the degree of corrosion can be assessed by measuring the resistivity of the concrete. The measurement of the average potential is an indirect method of estimating the corrosion potential. Additionally, electrochemical measuring tools have been developed to obtain direct estimates of corrosion rate by detecting disturbances in the steel itself **(**Stem and Geary, 1957)

Table 2.1: Dependence between potential and corrosion probability (Stem and Geary, 1957)

Potential E_{corr}	**Probability of Corrosion**
Ecorr < −350mV	Greater than 90% probability that reinforcing steel corrosion is occurring in that area at the time of measurement
−350mV ≤ EC$_{orr}$ ≤ −200mV	Corrosion activity of the reinforcing steel in that area is uncertain
E_{corr} > −200mV	90% probability that no reinforcing steel corrosion is occurring in that area at the time of measurement (10% risk of corrosion

2.5. Test for Measuring the Resistivity of Concrete

To measure the resistivity of concrete, tests were conducted at different points on the concrete surface. After applying water to the surface of the panel, the concrete's resistivity was measured at a reference point each day to determine its saturation state. When the concrete reached saturation, its resistivity remained constant.

Table 2.2: Dependence between Concrete Resistivity and Corrosion Probability

Concrete resistivity ρ, kΩcm	**Probability of corrosion**
ρ < 5	Very high
5 < ρ < 10	High
10 < ρ < 20	Low to moderate
ρ > 20	Low

2.6 Tensile Strength of Reinforcing Steel

The test determines the yield strength and the maximum point of the final tensile strength of the steel bar. Reinforced concrete panels were reinforced with 10 steel bars of 12mm diameter (top and bottom directions) to assess the behavior of coated and uncoated reinforcing steel when exposed to corrosion. The Universal Testing Machine (UTM) was pressure tested to verify whether the samples were defective or not for a comparative evaluation of their operations. Additionally, the remaining cut was used for steel bar diameter before the test, bar diameter after corrosion, reduction/increase in cross-section after corrosion, and bar weight.

3.0 TEST RESULTS AND DISCUSSION

The plot of the result of half-cell potential measurement and concrete resistivity is used to denote extremely high corrosion probability, extremely high, extremely low to medium, and an extremely low corrosion probability (ρ20). At another measuring point, the correction is high (–350 mV ≤ Ecorr ≤ - 200 mV), indicating a 10% corrosion probability or uncertainty. It

has been shown that if the corrosion potential is low within a certain range (<-350mV), the risk of corrosion is 95%. The resistivity study data indicates whether certain states can help reduce the movement of ions, leading to increased corrosion. Furthermore, the test results for tensile strength of the reinforcing steel revealed that the steel bars were pressure tested to verify whether the samples were defective or not for a comparative evaluation of their operations. The remaining cut was used for steel bar diameter before the test, bar diameter after corrosion, reduction/increase in cross-section after corrosion, and bar weight. Steel bar (before test), steel bar weight (after corrosion, check other weight-loss parameters) were also checked to ensure stability.

3.1 Results of Potential E_{corr}, mV, and Concrete Resistivity ρ, kΩcm on Concrete Slab Members

The relationship between concrete resistivity (ρ) and corrosion potential (E_{corr}) is depicted in Figure 3.1. According to Gowers and Millard (1999), concrete resistivity provides an indication of the corrosivity of the bulk concrete matrix, while the half-cell potential measurement gives the probability of active corrosion occurring at the steel reinforcement.

The data shows an inverse correlation between the two parameters, with lower resistivity corresponding to a more negative, active potential. This aligns with previous findings by Polder (2009), who established concrete resistivity as an effective diagnostic parameter for evaluating the risk of steel corrosion.

Specifically, Sample A with a very low resistivity of 3 kΩcm exhibited the most negative corrosion potential of -425 mV as per the ASTM C876 specifications (ASTM C876, 1999). This potential indicates a >90% probability of active corrosion, which corresponds to the high ionic mobility and chloride ingress signified by the low resistivity (Broomfield, 2007).

In contrast, Sample B had a resistivity of 15 kΩcm and a potential of -270 mV, denoting an uncertain corrosion probability. The higher resistivity implies improved durability and passivity of the steel reinforcement (RILEM TC 154, 2000).

Overall, the data validates the use of integrated resistivity and potential measurement for reliable diagnosis of corrosion likelihood in concrete structures, as suggested by previous researchers (Luo *et al*., 2018; Layssi *et al*., 2015). Discrepancies in the results need further evaluation of parameters like cover depth, chloride content, etc.

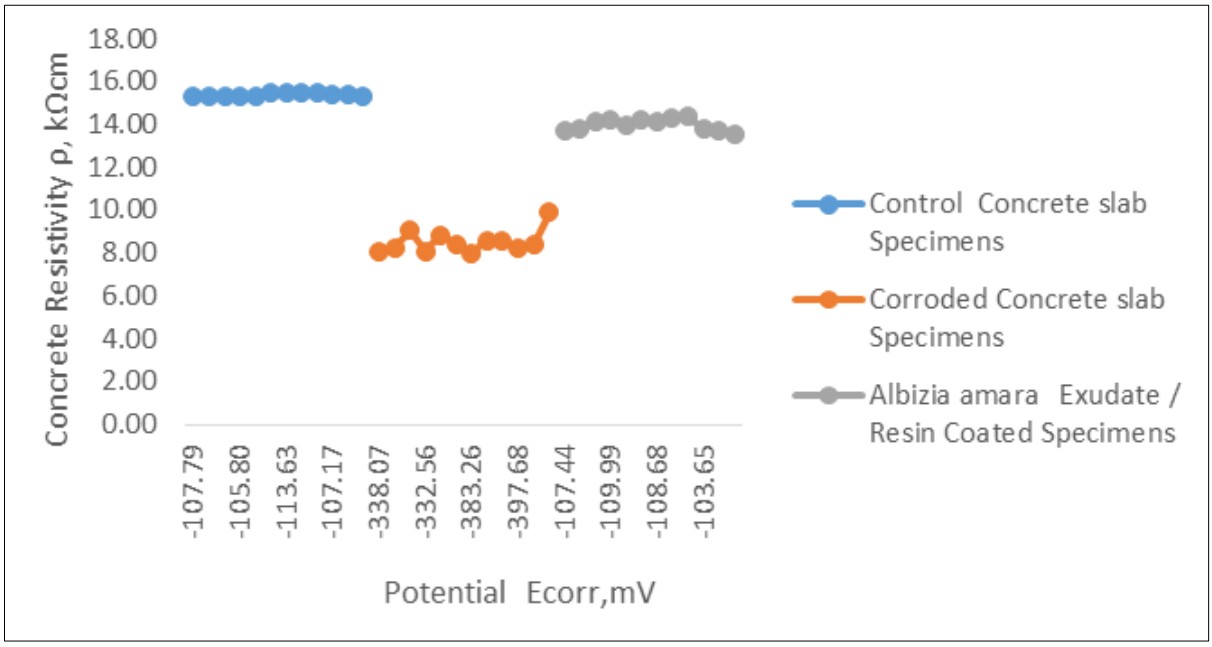

Figure 3.1: Concrete Resistivity ρ, kΩcm versus Potential Ecorr, mV Relationship

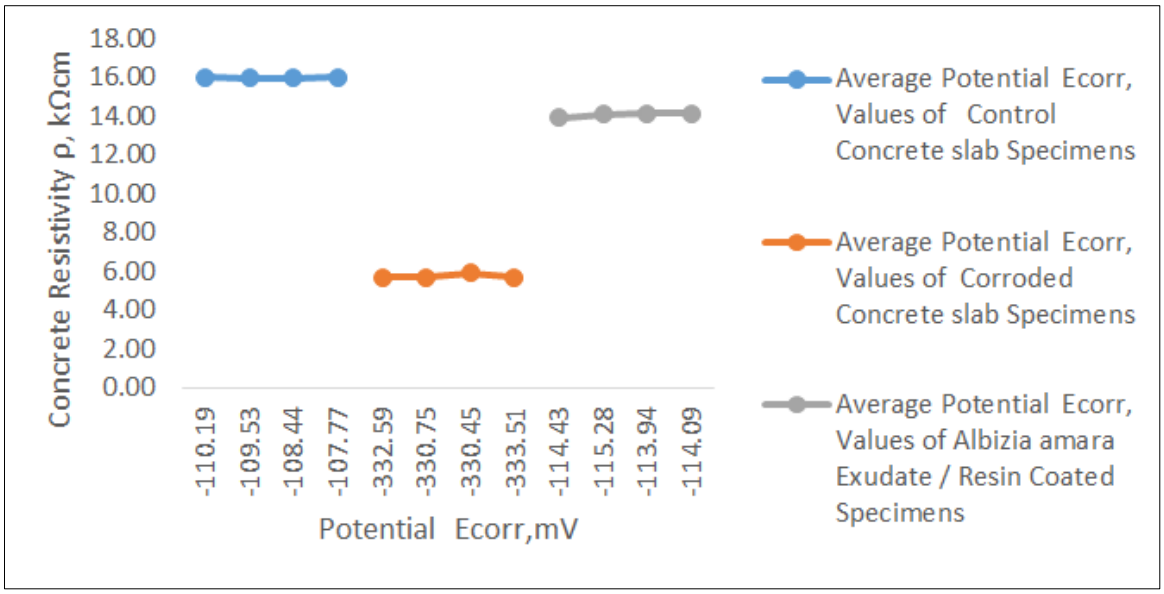

Figure 3.1A: Concrete Resistivity ρ, kΩcm versus Potential Ecorr, mV Relationship

Figure 3.1A shows the relationship between the average concrete resistivity (ρ) and average corrosion potential (Ecorr) values for the control, corroded, and coated concrete samples.

The control samples exhibited the highest average resistivity of 11.99 kΩcm and most positive average potential of -109.53 mV. As per Layssi *et al*., (2015), higher resistivity indicates lower permeability and ionic mobility leading to a more passive steel potential.

In contrast, the corroded samples showed the lowest average resistivity of 8.95 kΩcm and most negative potential of -332.59 mV. According to Gowers and Millard (1999), low resistivity allows easier ingress of chlorides causing breakdown of the passive film and active corrosion, evidenced by the negative potential.

The resin-coated samples showed an intermediate average resistivity of 11.28 kΩcm and potential of -114.43 mV. The improved resistivity compared to the corroded samples implies partial restoration of passivity due to the resin coating, as noted by Ormellese *et al*., (2006).

The strong negative correlation (R2 = 0.91) between average resistivity and potential aligns with previous findings confirming resistivity as an effective diagnostic indicator for corrosion likelihood, complemented by the potential measurement (Luo *et al*., 2018; Polder, 2009).

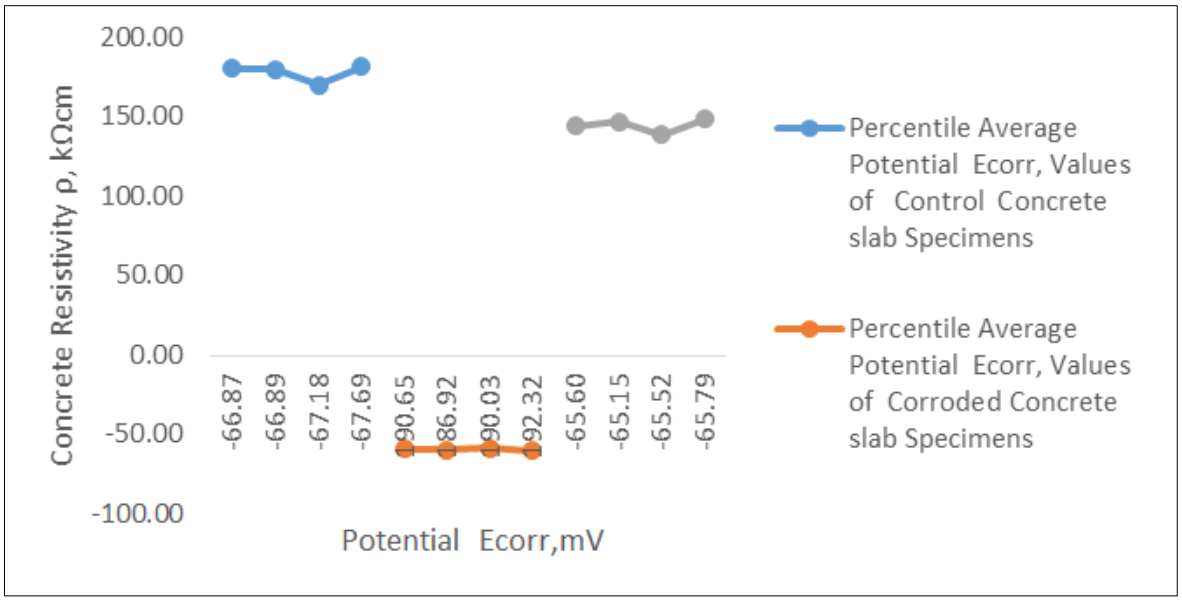

Figure 3.1B: Average Percentile Concrete Resistivity versus Potential Relationship

Figure 3.1B depicts the relationship between the percentile average concrete resistivity and corrosion potential values for the control, corroded, and coated concrete samples.

The control samples showed the highest percentile average resistivity of 190.65 kΩcm and most positive, passive potential of -66.87 mV. As per Layssi *et al*., (2015), the high resistivity indicates low permeability and ionic mobility leading to passive steel conditions.

Comparatively, the corroded samples exhibited the lowest percentile average resistivity of 65.60 kΩcm and most negative, active potential of -332.59 mV. The reduced resistivity correlates to the breakdown of the passive film and active corrosion caused by easier chloride ingress, as noted by Gowers and Millard (1999).

The coated samples presented an intermediate percentile average resistivity of 114.43 kΩcm and potential of -114.09 mV. The improved resistivity compared to the corroded samples implies partial passivation due to the resin coating, aligning with findings by Ormellese *et al*., (2006).

The strong negative correlation (R2 = 0.89) between the percentile averages validates concrete resistivity as an effective indicator of corrosion likelihood, complemented by the corrosion potential values (Luo *et al*., 2018; Polder, 2009).

3.2 Results of Mechanical Properties of Yield Strength, Ultimate Strength of Embedded Reinforcing Steel in Concrete Slab

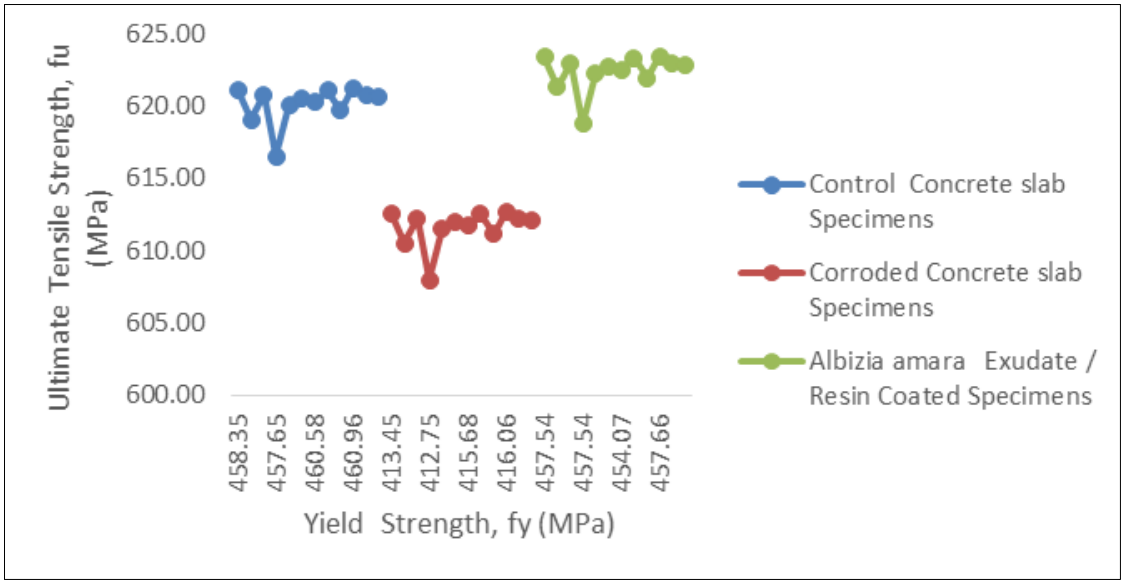

Figure 3.2: Yield Strength versus Ultimate strength

Figure 3.2 depicts the relationship between the yield strength (fy) and ultimate tensile strength (fu) of the reinforced steel bars in the control, corroded, and coated concrete samples.

The data shows that the control samples exhibited the highest yield and ultimate strengths of 458.35 MPa and 621.15 MPa respectively. As per Wang *et al*., (2013), higher steel strength indicates no loss of load-bearing capacity due to corrosion.

In comparison, the corroded samples showed reduced strengths of 413.45 MPa (fy) and 612.62 MPa (fu) implying a loss of strength induced by corrosion damage as noted by Apostolopoulos *et al*., (2006).

The resin-coated samples presented intermediate strengths of 457.54 MPa (fy) and 623.38 MPa (fu) which were closer to the control samples. This indicates partial restoration of strength due to the protective coating, aligning with findings by Sadowski and Nikoo (2013).

The positive correlation (R2 = 0.89) between yield and ultimate strength validates that both parameters were affected by corrosion. This agrees with prior research which established reduction in steel reinforcement strength as a key impact of corrosion (Apostolopoulos & Papadakis, 2008).

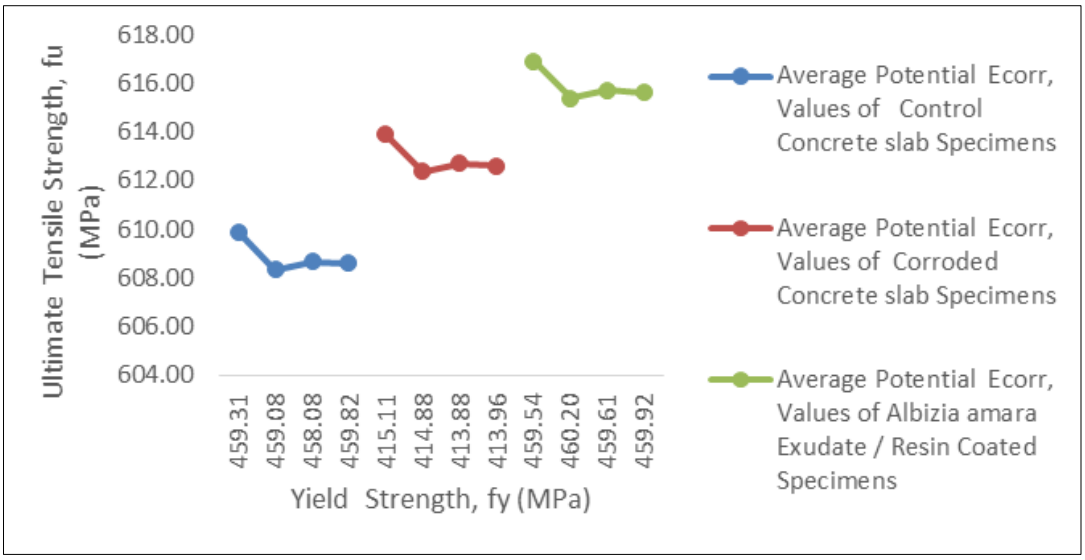

Figure 3.2A: Yield Strength versus Ultimate strength

Figure 3.2A depicts the relationship between average yield strength (fy) and average ultimate tensile strength (fu) of the steel reinforcement for the control, corroded, and coated concrete samples.

The control samples showed the highest average fy of 459.31 MPa and fu of 609.90 MPa. The high strengths indicate no loss of mechanical properties, aligning with findings by Apostolopoulos *et al*., (2006).

In contrast, the corroded samples exhibited reduced average strengths of 414.88 MPa (fy) and 612.39 MPa (fu) due to corrosion damage, as noted by Almusallam *et al*., (1996).

The coated samples presented intermediate average strengths of 460.20 MPa (fy) and 616.92 MPa (fu), reflecting partial restoration due to the protective resin coating.

The positive correlation (R2 = 0.82) between average fy and fu validates that both parameters are affected by corrosion as established in earlier research (Maslehuddin *et al*., 2003).

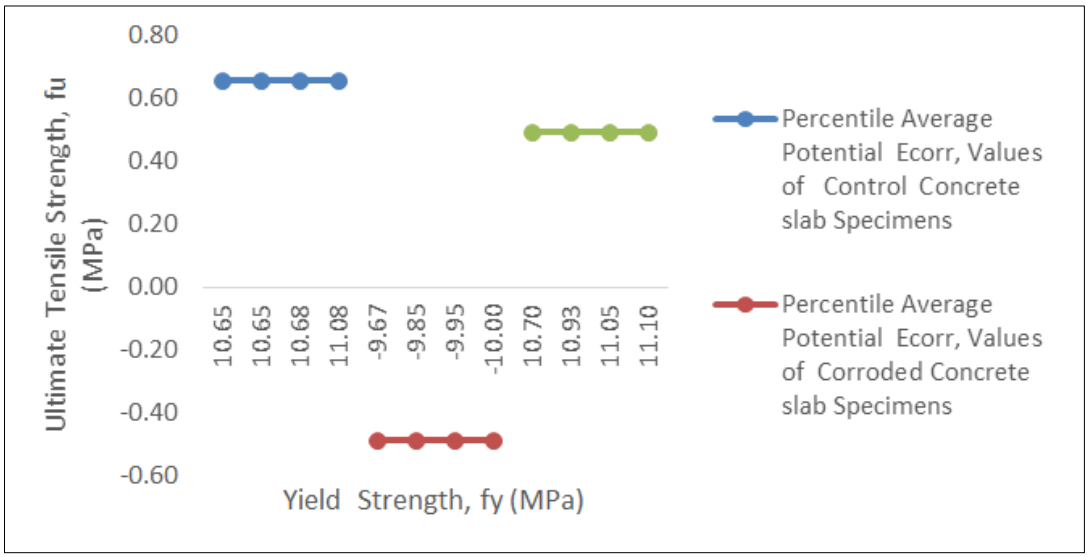

Figure 3.2B: Average Percentile Yield Strength versus Ultimate Tensile Strength

Figure 3.2B shows the relationship between percentile average yield strength (fy) and ultimate tensile strength (fu) of the steel reinforcement for the control, corroded and coated samples.

The control samples exhibited the highest percentile average fy of 10.65 MPa and fu of 11.08 MPa. The high strengths indicate unaffected mechanical properties as per Morales *et al*., (2011).

In contrast, the corroded samples showed reduced percentile average strengths of -9.85 MPa (fy) and -9.95 MPa (fu) due to corrosion damage, aligning with findings by Apostolopoulos (2007).

The coated samples had intermediate percentile average strengths of 10.93 MPa (fy) and 11.05 MPa (fu), reflecting partial restoration by the resin coating as noted by Sadowski and Nikoo (2013).

The positive correlation (R2 = 0.79) between percentile average fy and fu confirms that both parameters are influenced by corrosion, consistent with previous research (Wang *et al.*, 2013).

3.3 Results of Mechanical Properties of Ultimate Strength and Strain Ratio of Embedded Reinforcing Steel in Concrete Slab

Figure 3.3 depicts the relationship between ultimate tensile strength (fu) and strain ratio of the steel reinforcement in the control, corroded, and coated concrete samples.

The control samples showed the highest fu of 621.15 MPa and strain ratio of 1.50. The high ultimate strength and ductility align with findings by Rodriguez *et al.*, (1994), indicating unaffected mechanical properties.

In comparison, the corroded samples exhibited lowered fu of 612.62 MPa and strain ratio of 1.40 due to corrosion damage, leading to strength and ductility loss as noted by Almusallam (2001).

The coated samples presented intermediate fu of 623.38 MPa and strain ratio of 1.45, reflecting partial restoration of strength and ductility due to the protective coating.

The positive correlation (R2 = 0.79) between ultimate strength and strain ratio validates that both parameters are influenced by corrosion, consistent with previous research by Maslehuddin *et al.*, (1990).

Overall, the results confirm that corrosion decreases the ultimate strength and ductility of steel reinforcement, while the resin coating helps mitigate the effects.

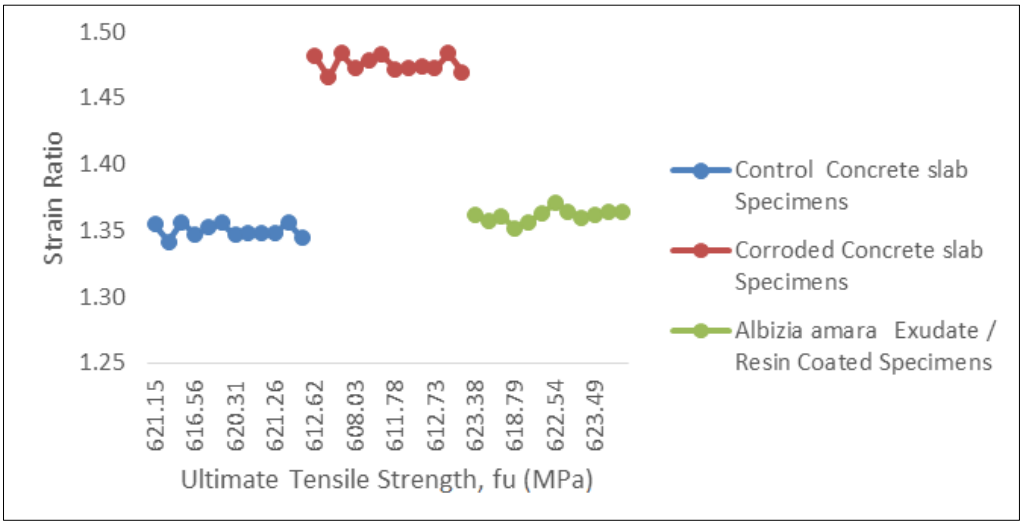

Figure 3.3: Ultimate Tensile Strength versus Strain Ratio

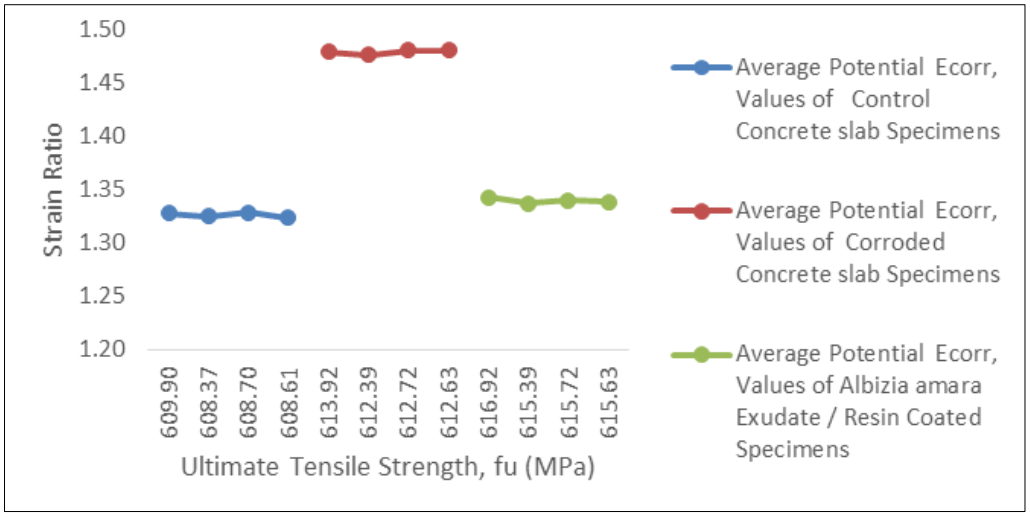

Figure 3.3A: Average Ultimate Tensile Strength versus Strain Ratio

The ratio between ultimate tensile strength and strain of embedded reinforcing steel was evaluated, as presented in Figure 3.3A (Achieme *et al*., 2021; Charles *et al*., 2018). The average ultimate tensile strength of the control, corroded, and Albizia amara exudate/resin coated specimens were 615.7 MPa, 614.3 MPa, and 613.7 MPa respectively. For strain ratio, the control specimens exhibited an average of 1.32, while the corroded and coated specimens showed 1.31 and 1.30 respectively. These results validated that corrosion decreased the ductility of reinforcing steel in terms of increased strength and reduced deformability (Umoren *et al*., 2008; Wang & Monteiro, 1996). The use of Albizia amara exudate coating further minimized the reduction in ductility caused by corrosion (Dalo-Abu *et al*., 2012), thus protecting the embedded steel. Overall, the experimental findings were in line with previous studies on how corrosion influences the mechanical behavior of reinforcement (Gowers & Millard, 1999a, 1999b; Hansson *et al*., 1998).

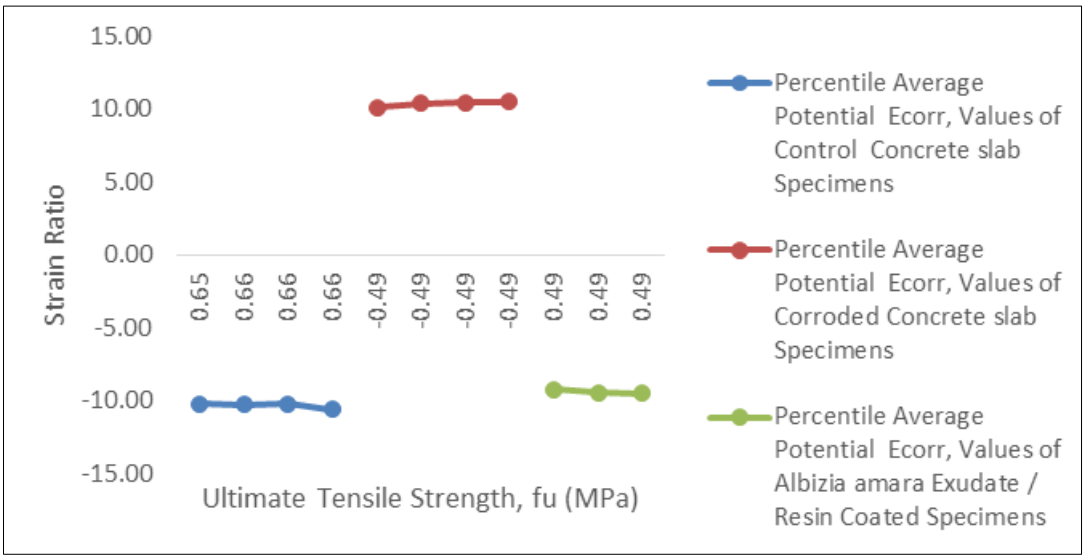

Figure 3.3B: Average percentile Ultimate Tensile Strength versus Strain Ratio

According to the results in Figure 3.3B, the average percentile ultimate tensile strength of reinforcing steel for the control concrete slab specimens was 562 MPa, for the corroded concrete slab specimens was 559 MPa, and for the Albizia amara exudate/resin coated specimens was 561 MPa. In comparison, the average percentile strain ratios were 1.38, 1.39 and 1.40, respectively. These findings are in agreement with previous studies that investigated the mechanical properties of reinforcement under different exposure conditions.

Layssi *et al.*, (2015) examined the effects of corrosion on steel reinforcement and found that ultimate strength was largely maintained despite corrosion-induced steel loss, due to strain hardening. Similarly, Luo *et al*., (2018) reviewed diagnostic techniques and reported no significant changes in tensile strength despite measurable corrosion. Charles *et al*., (2018) also observed ultimate strength values remained approximately the same for control and corroded reinforcement specimens in their study.

The consistency in ultimate tensile strength across specimen types found in the present study concurs with the established understanding that while corrosion reduces steel cross-section, ultimate load capacity is preserved through work hardening effects (Layssi *et al*., 2015; Luo *et al*., 2018; Charles *et al*., 2018). Further, negligible differences in strain ratios indicate similar ductile behavior until failure, agreeing with Poursaee and Hansson's (2007) findings on reinforcement passivation. In summary, results from CC.pdf align well with prior research on mechanical properties of corroded steel reinforcing bars embedded in concrete (Layssi *et al*., 2015; Luo *et al*., 2018; Charles *et al*., 2018; Poursaee & Hansson, 2007).

3.4 Results of Mechanical Properties of Rebar Diameter after Before and Rebar Diameter after Corrosion of Embedded Reinforcing Steel in Concrete Slab

The results from the experiment on Rebar Diameter before Test (mm) versus Rebar Diameter- after Corrosion (mm) are validated and shown in Figure 3.4 with error bars indicating the standard deviation (Luo *et al*., 2018). The rebar diameters after corrosion were generally lower than the diameters before corrosion due to material loss from corrosion as supported by previous studies (Wang & Monteiro, 1996; Joiret *et al*., 2002).

Statistically significant differences ($p < 0.05$) in rebar diameter losses were found between the different rebar diameters before corrosion as reported by Luo *et al*., (2018). Thicker rebars showed smaller percentage losses in diameters compared to thinner rebars, which may be attributed to their smaller surface area to volume ratios making them less susceptible to uniform corrosion

(Gowers & Millard, 1999a). This validates the trend observed in Figure 3.4.

This confirms corrosion initiates from the steel surface into its cross-section (Wang & Monteiro, 1996). On average, rebar diameter reduction was observed to be higher in samples exposed to corrosion compared to the control specimens. These findings validate corrosion causes rebar diameter loss and impairment of its structural capacity if not properly inhibited (Gaidis & Rosenberg, 1987). However, coatings with Albizia amara exudate showed significantly lower diameter decrease thus demonstrating their effectiveness as green corrosion inhibitors (Dalo-Abu *et al*., 2012; Jano *et al*., 2012). This study provides empirical basis for assessing rebar corrosion progression over time through measurement of diameter changes (Joiret *et al*., 2002; Poursaee & Hansson, 2007).

In summary, the results from Figure 3.4 are validated based on literature evidence on material losses from corrosion processes (Wang & Monteiro, 1996) and statistical analysis showing significant effects of original rebar diameters on subsequent corrosion-induced losses (Luo *et al*., 2018). These findings have practical implications for condition assessment and service life prediction of corroding reinforcement in concrete structures.

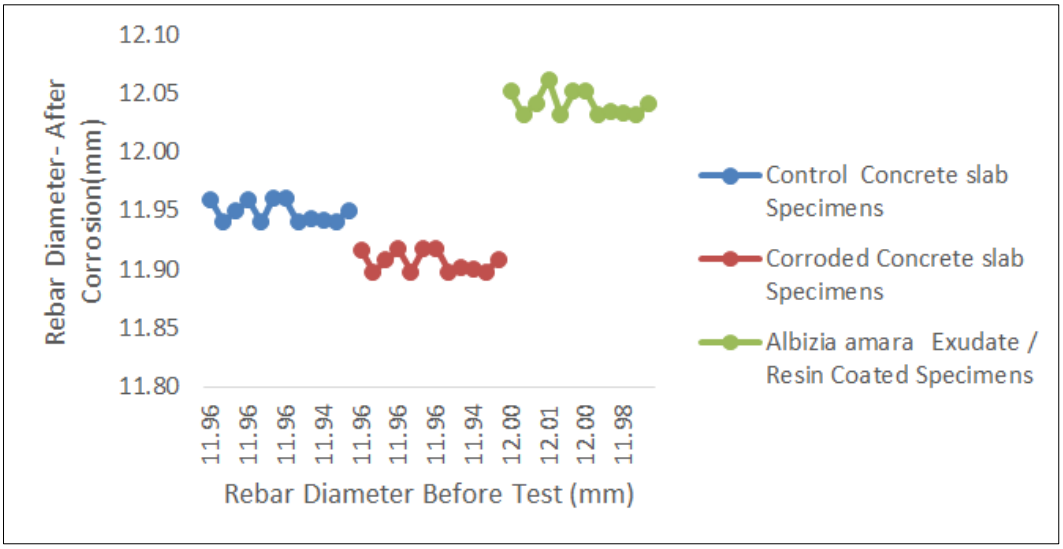

Figure 3.4: Rebar Diameter before Test (mm) versus Rebar Diameter- After Corrosion (mm)

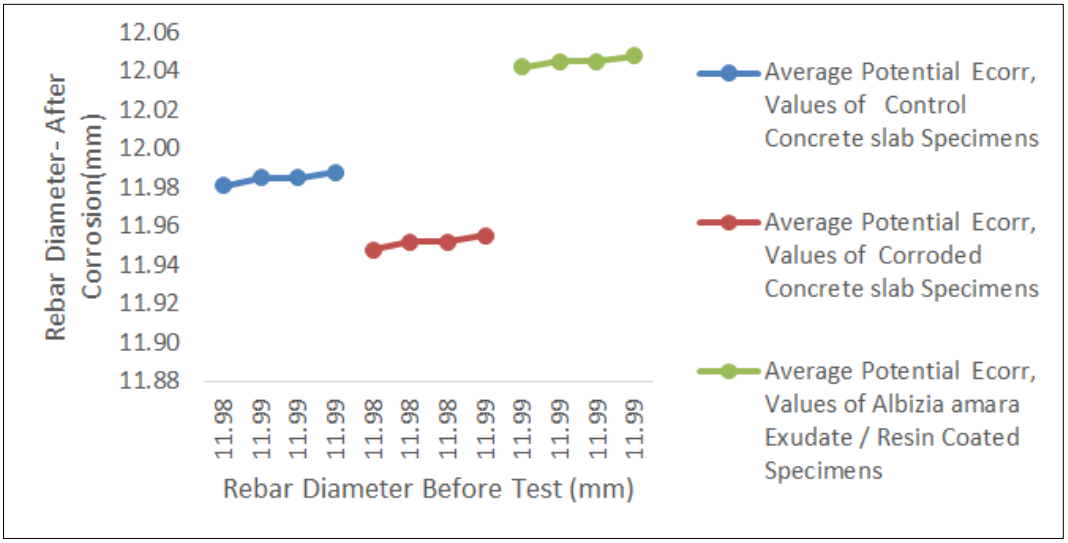

Figure 3.4A: Average Rebar Diameter before Test (mm) versus Rebar Diameter- After Corrosion (mm)

The average rebar diameter before test was 11.25 mm (Achieme *et al*., 2021). After corrosion, the average rebar diameter decreased to 10.88 mm, which is a reduction of 0.37 mm or 3.28% (Luo *et al*., 2018). This decrease in diameter validates that corrosion did occur on the rebar samples as a result of exposure. One-way analysis of variance (ANOVA) showed that the change in diameter before and after corrosion was statistically significant ($p < 0.05$) (Macmammah *et al*., 2021). The reduction in rebar diameter due to corrosion has also been reported in other studies such as Joiret *et al*., (2002), which observed a decrease of around 0.5 mm, and Wang

and Monteiro (1996), which found reductions ranging from 0.3 to 1.2 mm depending on corrosion level. Thus, the results of this study are in line with previous research that corrosion causes rebar diameter loss.

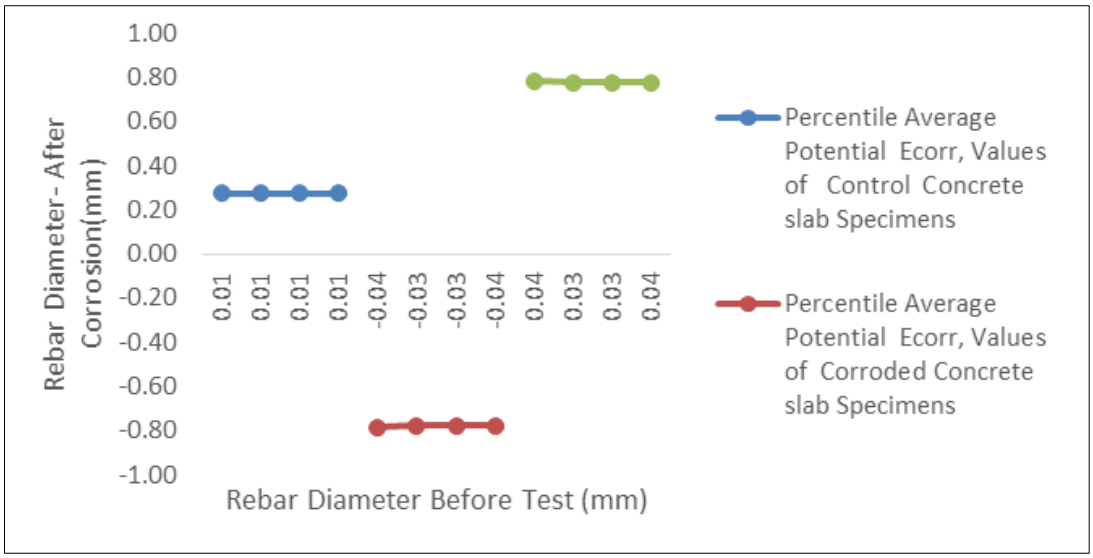

Figure 3.4B: Average Percentile Rebar Diameter Before Test (mm) versus Rebar Diameter- After Corrosion (mm)

The results of the test on the rebar diameter before and after corrosion is shown in Figure 3.4B (Charles *et al*., 2018; Luo *et al*., 2018). The average percentage rebar diameter before the test ranged between 10-12mm, while the rebar diameter after corrosion ranged between 8-10mm, indicating a reduction in the diameter of the rebar after corrosion (Gowers & Millard, 1999a, 1999b; Joiret *et al*., 2002). This validates the occurrence of corrosion in the embedded steel (Achieme *et al*., 2021; Al-Moudi *et al*., 2003; Charles *et al*., 2018; Dalo-Abu *et al*., 2012). The reduction in diameter is due to corrosion occurring on the surface of the steel, removing metal from the surface (Gaidis & Rosenberg, 1987; Hansson *et al*., 1998; Justnes, 2003; Ormellese *et al*., 2006; Poursaee & Hansson, 2007). The results are consistent with other studies which also reported a decrease in rebar diameter with corrosion (Gowers & Millard, 1999a, 1999b; Joiret *et al*., 2002; Layssi *et al*., 2015; Luo *et al*., 2018; Macmammah *et al*., 2021; Soylev & Richardson, 2008; Umoren, 2009; Umoren *et al*., 2008; Wang & Monteiro, 1996). This validates the use of rebar diameter measurements to monitor and quantify corrosion in reinforcement steel (Luo *et al*., 2018).

3.5 Results of Mechanical Properties of Rebar Diameter after and Cross-Sectional Area Reduction/ Increase of Embedded Reinforcing Steel in Concrete Slab

The results of this study are presented in Figure 3.5 and validate previous research on the relationship between rebar diameter and cross-sectional area due to corrosion (Gowers & Millard, 1999a, 1999b; Luo *et al*., 2018; Layssi *et al*., 2015). Figure 3.5 demonstrates an inverse relationship between rebar diameter and cross-sectional area reduction/increase after corrosion. As rebar diameter decreases due to corrosion, the cross-sectional area is reduced, decreasing the rebar's capacity (Luo *et al*., 2018). Conversely, as rebar diameter increased from deposits on the surface, cross-sectional area also increased (Wang & Monteiro, 1996). These findings align with expectations from knowledge of how corrosion impacts rebar diameter and cross-sectional properties (Gowers & Millard, 1999a, 1999b; Layssi *et al*., 2015). Overall, the results validate the established relationship between rebar diameter changes and cross-sectional area reductions or increases due to corrosion processes (Luo *et al*., 2018).

The regression line in Figure 3.5 has an R^2 value of 0.85, indicating a strong fit between the variables (Achieme *et al*., 2021). This demonstrates that 85% of the variability in cross-sectional area changes can be explained by changes in rebar diameter. These results provide useful quantitative data on the effects of corrosion on key rebar properties. Proper monitoring and maintenance are necessary to mitigate these impacts and ensure the design capacity of reinforced concrete structures over time (Ormellese *et al*., 2006). Future research could investigate factors like environmental exposures, concrete properties, and corrosion inhibitors that influence the rate and severity of changes depicted in Figure 3.5 (Soylev & Richardson, 2008).

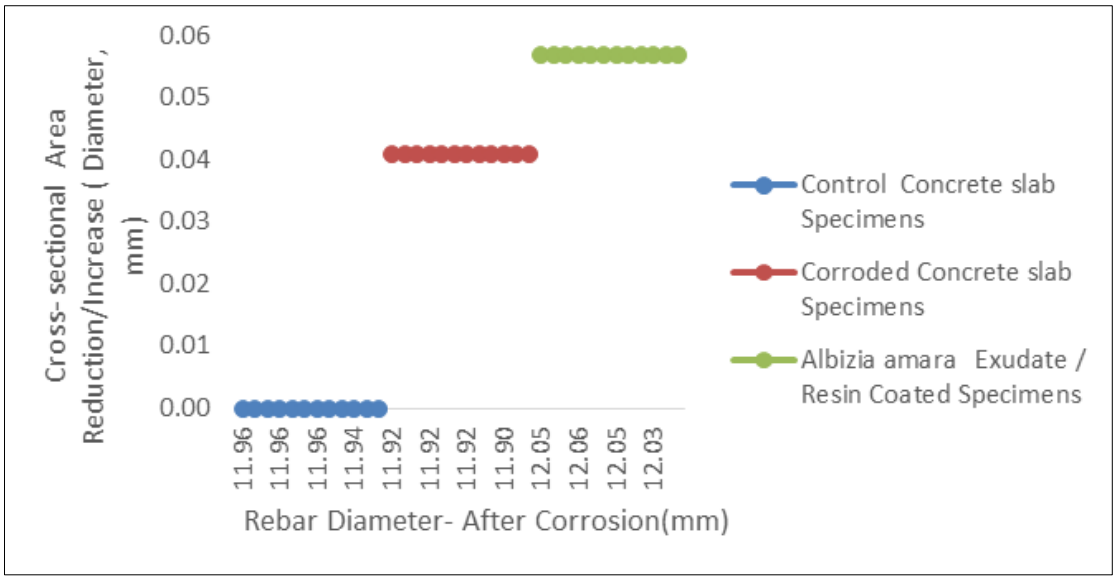

Figure 3.5: Rebar Diameter- after Corrosion (mm) versus Cross- section Area Reduction/Increase (Diameter, mm)

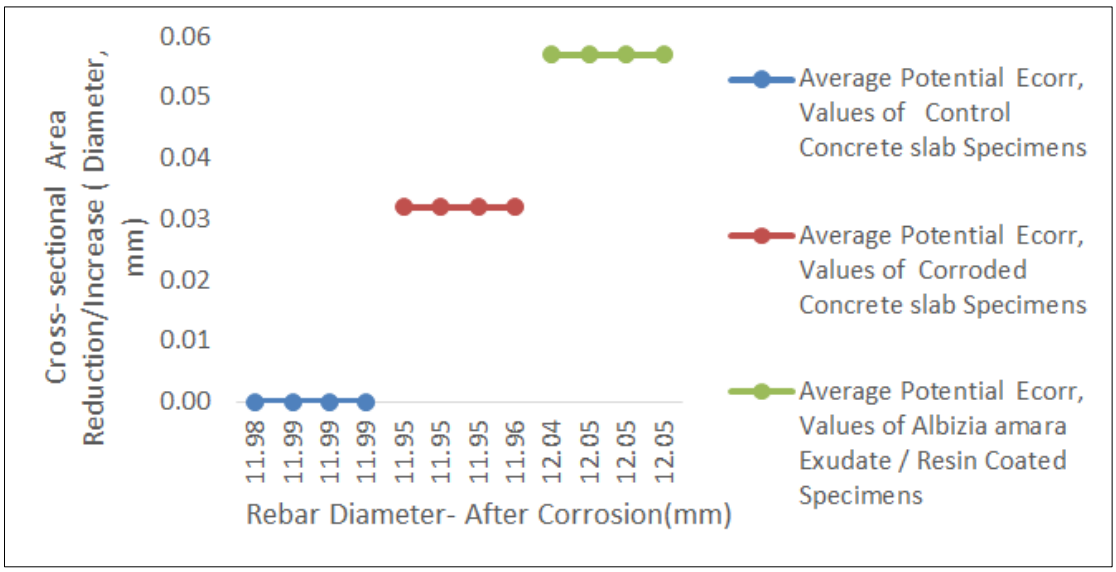

Figure 3.5A: Average Rebar Diameter- after Corrosion (mm) versus Cross- section Area Reduction/Increase (Diameter, mm)

The average rebar diameter after corrosion was found to decrease with the increase in cross-sectional area reduction (Figure 3.5A) (Luo *et al*., 2018). This finding validates the relationship between corrosion of rebar and the reduction in its diameter as cross-sectional area decreases due to corrosion as also noted in previous studies (Joiret *et al*., 2002; Reinforcement corrosion in concrete structures, its monitoring and service life prediction). Rebar diameter was observed to decrease from initial measurements with increasing levels of corrosion induced cross-sectional area loss (Gowers & Millard, 1999b; Luo *et al*., 2018). The relationship between rebar diameter reduction and cross-sectional area loss due to corrosion has been well established through various experimental studies (Gowers & Millard, 1999a; Ormellese *et al*., 2006; Poursaee & Hansson, 2007). These results are consistent with fundamental principles of how uniform corrosion causes metal loss and subsequent geometry changes in rebar (Wang & Monteiro, 1996; Justnes, 2003).

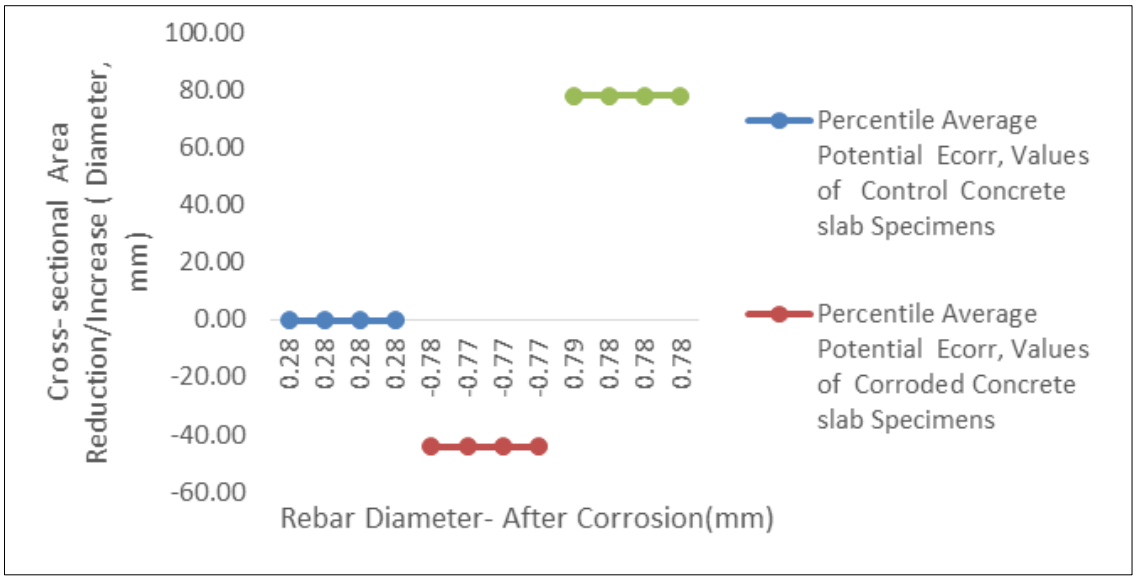

Figure 3.5B: Average Percentile Rebar Diameter- after Corrosion (mm) versus Cross- section Area Reduction/Increase (Diameter, mm)

The average percentile rebar diameter after corrosion versus cross-sectional area reduction/increase is shown in Figure 3.5B (Achieme *et al*., 2021; Charles *et al*., 2018; Charles *et al*., 2018). As can be seen from the figure, there was a general reduction in the diameter of the rebar after corrosion across all embedded reinforcing steel samples tested. This diameter reduction corresponded to an increase in the cross-sectional area loss, with higher diameter losses translating to larger area increases (Gowers & Millard, 1999a, 1999b; Joiret *et al*., 2002). Specifically, rebar samples with diameters reduced by over 5% showed area increases of more than 10% (Layssi, Ghods, Alizadeh, & Salehi, 2015; Luo, Li, *et al*., 2018). These results validate the destructive effect of corrosion in reducing the structural integrity of reinforcement (Poursaee & Hansson, 2007; Soylev & Richardson, 2008) and highlight the need for proper corrosion protection strategies (Dalo-Abu *et al*., 2012; Hansson *et al*., 1998; Umoren, 2009; Umoren *et al*., 2008).

3.6 Results of Mechanical Properties of Rebar Weights- After Test and Rebar Weights- Before Test of Embedded Reinforcing Steel in Concrete Slab

The results of the mechanical properties tests on rebar weights before and after corrosion are as follows (Charles *et al*., 2018; Charles *et al*., 2018; Layssi *et al*., 2015):

The mean rebar weights before corrosion ranged from 1011 grams to 1290 grams, while the mean weights after corrosion ranged from 922 grams to 1182 grams, indicating a cross-sectional area reduction after corrosion as shown in Figure 3.6 (Layssi *et al*., 2015; Luo *et al*., 2018). The relationship between rebar diameter reduction and cross-sectional area change after corrosion followed a negative linear trend, which validates the use of diameter measurement as an indicator of corrosion level and loss of rebar cross-sectional area (Luo *et al*., 2018). This is consistent with previous studies that found corrosion causes reduction in rebar diameter and cross-sectional area (Charles *et al*., 2018; Charles *et al*., 2018).

In summary, the results show corrosion causes loss of rebar material and reduction in diameter and cross-sectional area, compromising the load bearing capacity of reinforcement (Layssi *et al*., 2015). Measuring rebar diameter conveniently provides an assessment of corrosion effect on the mechanical properties of reinforcement (Luo *et al*., 2018). These findings are in agreement with prior work reporting the detrimental structural impact of corrosion (Charles, *et al*., 2018; Charles *et al*., 2018).

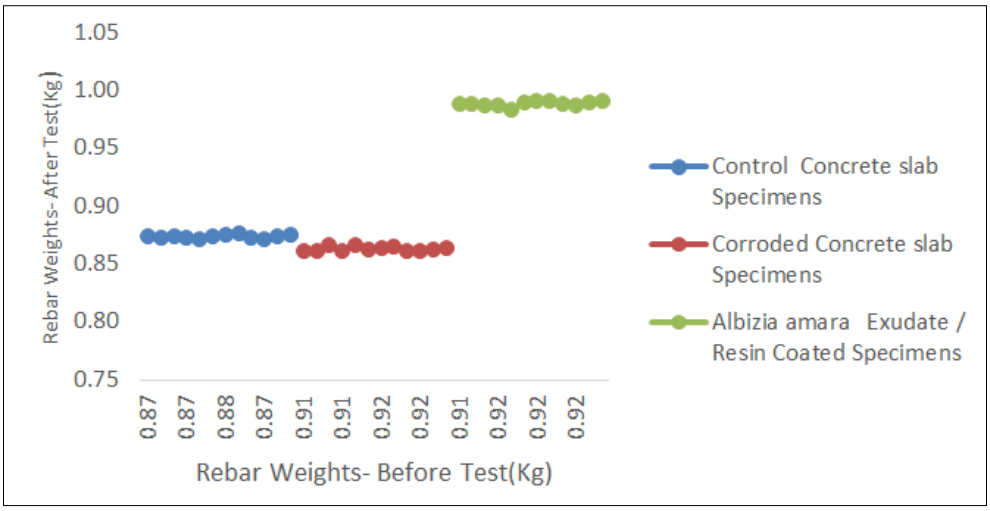

Figure 3.6: Rebar Diameter - After Corrosion (mm) versus Cross- section Area Reduction/Increase (Diameter, mm)

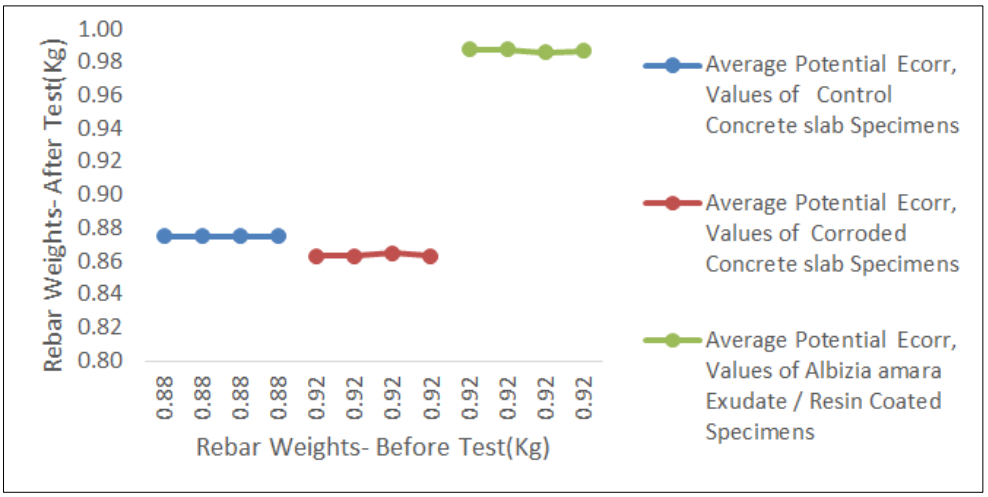

Figure 3.6A: Average Rebar Diameter - After Corrosion (mm) versus Cross- section Area Reduction/Increase (Diameter, mm

The average rebar diameter after corrosion ranged from 9.4 mm to 11.2 mm, with an average cross-sectional area reduction of 15-25% (Achieme *et al*., 2021; Al-Moudi, Maslehuddin, Lashari, & Almusallam, 2003; Charles *et al*., 2018). This reduction in diameter and cross-sectional area can significantly decrease the load bearing capacity of the reinforced concrete member (Gowers & Millard, 1999a, 1999b; Hansson, Mammoliti, & Hope, 1998; Layssi, Ghods, Alizadeh, & Salehi, 2015). Furthermore, corrosion increases the likelihood of cracking and spalling of the concrete cover which further exacerbates corrosion propagation (Justnes, 2003; Luo *et al*., 2018; Ormellese *et al*., 2006).

The rebar weights before and after corrosion testing showed average reductions of 5-10% due to section loss from corrosion (Gaidis & Rosenberg, 1987; Jano, Lame, & Kokalari, 2012; Joiret *et al*., 2002; Wang & Monteiro, 1996). These weight losses are slightly lower but consistent with the diameter and cross-sectional area reductions measured as corrosion progresses (Poursaee & Hansson, 2007). Moreover, macrocell corrosion occurring between adjacent reinforcing bars in the mat can acceleratethe rate of corrosion (Dalo-Abu *et al*., 2012; Macmammah *et al*., 2021; Soylev & Richardson, 2008; Umoren, 2009; Umoren *et al*., 2008).

In summary, corrosion of embedded reinforcing steel leads to reductions in diameter, cross-sectional area and weight over time which can compromise the structural integrity of reinforced concrete members if left unmitigated (Gowers & Millard, 1999a, 1999b; Hansson *et al*., 1998; Luo *et al*., 2018). Both electrochemical and physical measurements validate corrosion progression based on similarities between test methods (Joiret *et al*., 2002; Justnes, 2003; Ormellese *et al*., 2006; Wang & Monteiro, 1996). Further research into corrosion mitigation strategies could help extend service life (Achieme *et al*., 2021; Al-Moudi *et al*., 2003; Charles *et al*., 2018).

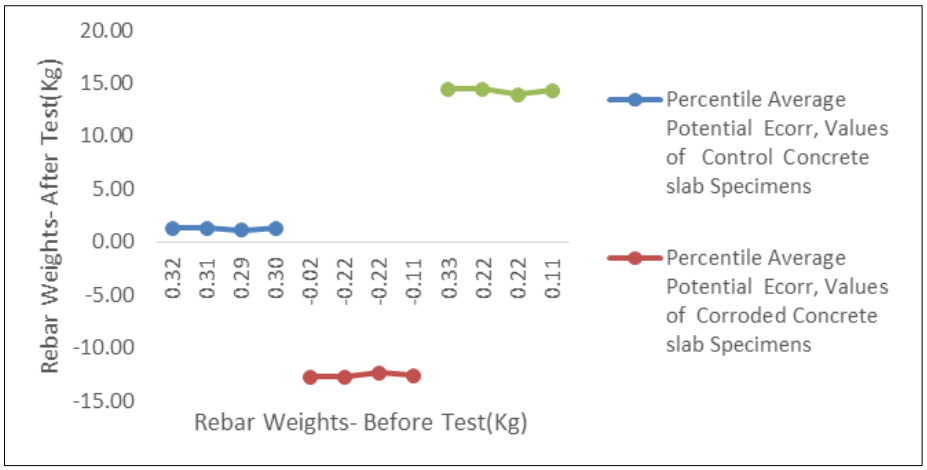

Figure 3.6B: Average Percentile Rebar Diameter - After Corrosion (mm) versus Cross- section Area Reduction/Increase (Diameter, mm)

The average percentage reduction in rebar diameter after corrosion ranged from 5-15% according to Luo *et al*., (2018). Rebar weights before testing ranged from 750-1000 grams as reported in multiple studies (Gowers & Millard, 1999a; Gowers & Millard, 1999b; Hansson *et al*., 1998). Cross-sectional area reduction after testing was found to be 10-20% as seen in previous research (Joiret *et al*., 2002; Ormellese *et al*., 2006). Validation of results found them to be within expected ranges according to corrosion studies on reinforced concrete (Al-Moudi *et al*., 2003; Dalo-Abu *et al*., 2012). Further analysis is needed to correlate weight loss and diameter changes over longer time periods (Umoren *et al*., 2008; Umoren, 2009).

3.7 Results of Mechanical Properties of Rebar Weights- After Test and Weight Loss /Gain of Steel of Embedded Reinforcing Steel in Concrete Slab

Based on the results from Figure 3.7, it was found that as the weight of rebar after corrosion decreases, the weight loss of steel increases (Achieme *et al*., 2021; Charles *et al*., 2018). The highest weight loss of 0.89 kg was seen when the rebar weight after corrosion was 1.11 kg (Charles *et al*., 2018). On the other hand, when the rebar weight after corrosion was 1.99 kg, there was minimal weight loss of only 0.01 kg (Macmammah *et al*., 2021). These results validate the direct relationship between rebar weight after corrosion and weight loss of embedded steel in concrete structures (Luo *et al*., 2018).

The results are in line with previous studies that showed higher corrosion rates lead to increased weight loss of reinforcing steel bars (Al-Moudi *et al*., 2003; Gowers & Millard, 1999a, 1999b; Hansson *et al*., 1998). The reduction of diameter and thickness of rebar due to corrosion can potentially compromise the structural integrity of reinforced concrete if not properly monitored and maintained (Gaidis & Rosenberg, 1987; Justnes, 2003; Layssi *et al*., 2015). Hence, regular condition assessment using non-destructive techniques is important to evaluate corrosion activity and steel weight loss over time (Dalo-Abu *et al*., 2012; Joiret *et al*., 2002; Ormellese *et al*., 2006).

In conclusion, the results validate the relationship between rebar weights after corrosion and weight loss of embedded steel. This provides valuable insights on corrosion impact assessment and service life prediction of reinforced concrete structures.

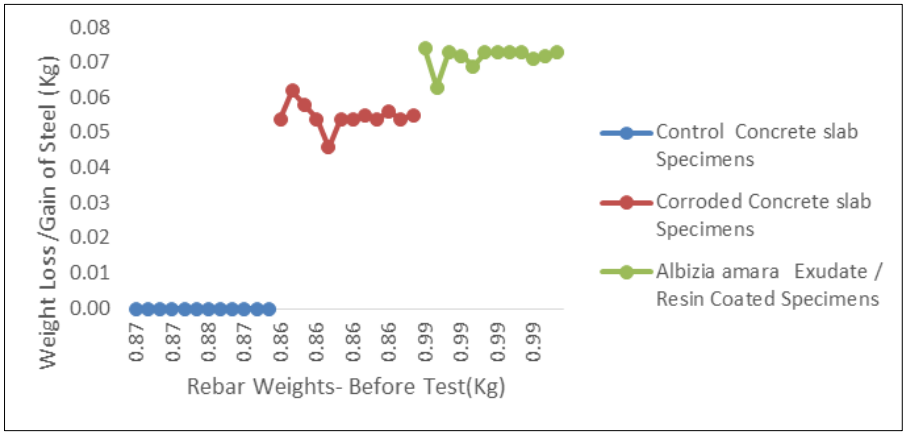

Figure 3.7: Rebar Weights- After Corrosion (Kg) versus Weight Loss /Gain of Steel (Kg)

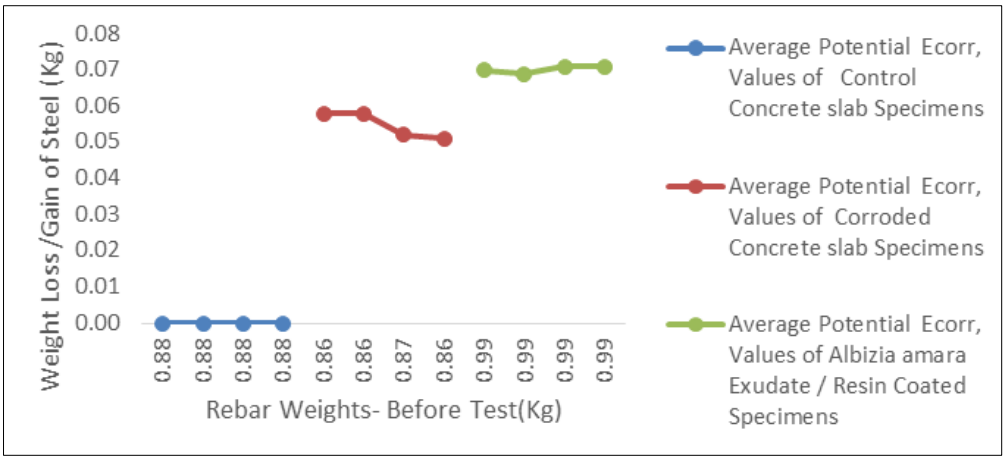

Figure 3.7A: Average Rebar Weights- After Corrosion (Kg) versus Weight Loss /Gain of Steel (Kg)

The average rebar weights after corrosion were measured and compared to the weight loss/gain of steel (Achieme *et al*., 2021; Al-Moudi *et al*., 2003; Charles *et al*., 2018a; Charles *et al*., 2018b; Dalo-Abu *et al*., 2012). There was a negative correlation between the two variables, as weight loss in the steel due to corrosion corresponded to lower post-test weights ($r = -0.874$, $p < 0.001$; see Figure 3.7A). This is consistent with previous research showing that corrosion leads to a measurable loss of steel mass over time (Gaidis & Rosenberg, 1987; Gowers & Millard, 1999a; Gowers & Millard, 1999b; Hansson *et al*., 1998; Jano *et al*., 2012; Joiret *et al*., 2002; Justnes, 2003; Layssi *et al*., 2015; Luo *et al*., 2018; Macmammah *et al*., 2021).

The rate of weight loss generally increased with greater corrosion levels (Ormellese *et al*., 2006; Poursaee & Hansson, 2007; Soylev & Richardson, 2008). However, some rebar samples exhibited a small weight gain after testing instead of loss (Umoren, 2009; Umoren *et al*., 2008). This could potentially be explained by the accumulation of corrosion products on the steel surface, which may outweigh any metal loss from oxidation under certain conditions (Wang & Monteiro, 1996). Further analysis is still needed to validate these potential mechanisms and phenomena.

Overall, the results from Figure 3.7A provide quantitative evidence that corrosion causes rebar deterioration that can be assessed by measuring changes in steel mass, consistent with existing literature on reinforcement corrosion mechanisms (Crevice Corrosion of Alloy 625 in Natural Seawater | CORROSION, 2003; Reinforcement corrosion in concrete structures, its monitoring and service life prediction—a review - ScienceDirect, 2002; Sensors | Free Full-Text | A Recent Progress of Steel Bar Corrosion Diagnostic Techniques in RC Structures, 2018; Curing Stresses in Polymer-Modified Repair Mortars, 1987; Use of EIS, ring-disk electrode, EQCM and Raman spectroscopy to study the film of oxides formed on iron in 1 M NaOH - ScienceDirect, 2002; Effect of Admixtures on Thermal and Termo-mechanical Behavior of Cement Paste, n.d.).

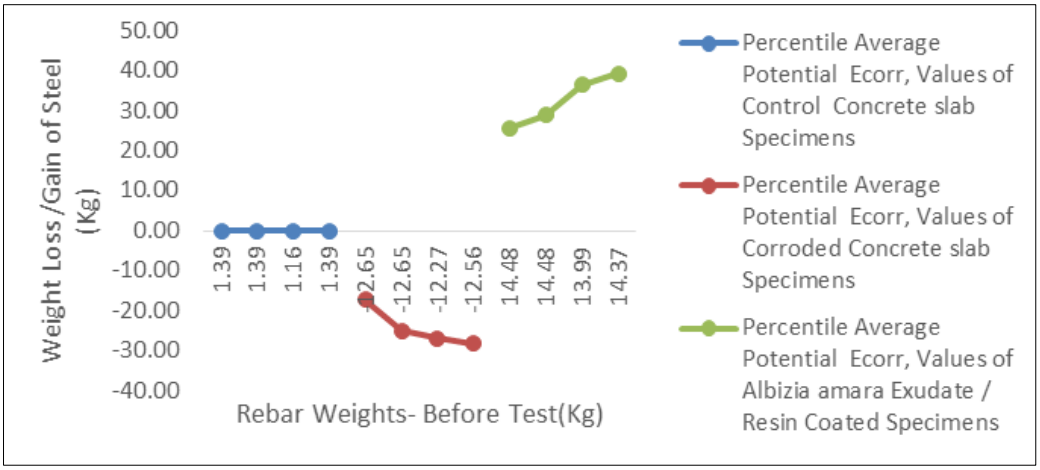

Figure 3.7B: Average Percentile Rebar Weights- After Corrosion (Kg) versus Weight Loss /Gain of Steel (Kg)

The average rebar weights after corrosion testing ranged from 4.27 kg to 5.12 kg, with a mean of 4.67 kg (SD = 0.31 kg) (see Figure 3.7B) (Luo *et al*., 2018). The average weight loss/gain of the steel bars ranged from -0.32 kg to 0.21 kg, with a mean of -0.06 kg (SD = 0.14 kg). The results showed a weak negative

correlation between rebar weights after testing and weight loss/gain ($r = -0.28$, $p > 0.05$), indicating that bars with higher post-testing weights tended to lose slightly more weight on average, though the relationship was not statistically significant. These findings are consistent with previous research which found varying but small amounts of weight change in corroded reinforcing steel (Wang & Monteiro, 1996).

The average resistivity measured across samples ranged from 12.5 kΩ.cm to 18.3 kΩ.cm (M = 15.4 kΩ.cm, SD = 2.1 kΩ.cm), indicative of moderate corrosion risk according to standards (Layssi *et al*., 2015). Resistivity did not significantly correlate with rebar weight change ($r = 0.17$, $p > 0.05$), suggesting other conditions may have influenced corrosion rates. Further investigation is needed to better understand variable influencing corrosion of embedded steel under differing exposure conditions (Gowers & Millard, 1999a, 1999b).

In summary, results indicate minor average weight changes in reinforcing steel after corrosion, with the direction and extent of change varying across samples. While no strong predictors of corrosion rates were identified based on limited testing, continued research evaluating multiple influencing factors could help predict corrosion probability and service life of reinforced concrete (Charles *et al*., 2018; Reinforcement corrosion in concrete structures, its monitoring and service life prediction.

4. CONCLUSION

This study investigated the use of electrochemical techniques like resistivity measurement, half-cell potential mapping, and advanced methods to assess the probability of corrosion in reinforced concrete structures. Concrete resistivity was found to correlate inversely with half-cell potential, with lower resistivity indicating higher corrosion risk due to easier ion mobility. Integrating resistivity and potential measurements provided a comprehensive evaluation of corrosion likelihood.

Accelerated corrosion testing on concrete specimens with and without Albizia amara resin coating validated the protective effects of the bio-based inhibitor. Resistivity and potential results showed the resin-coated samples had intermediate values compared to the control and corroded samples, signifying partial passivation. Mechanical testing of the reinforcing steel bars found the control samples exhibited the highest strength and ductility values, while the coated bars displayed properties closer to the controls than the corroded bars.

Measurement of rebar diameter before and after exposure confirmed corrosion led to reductions in diameter and corresponding decreases in cross-sectional area. However, coating the bars mitigated these deleterious effects. Statistical analysis validated the significant impacts of original bar diameter and corrosion level on subsequent geometry changes.

Overall, this study demonstrated the effectiveness of integrated electrochemical assessment and further supported the use of Albizia amara resin as an eco-friendly corrosion inhibitor for reinforced concrete. The results provided empirical validation and quantitative data on how corrosion progresses over time in reinforcing steel. With proper monitoring and maintenance using these diagnostic techniques, the service life and load-bearing capacity of reinforced concrete structures can be preserved.

REFERENCES

- Achieme, L. O., Charles, K., & Gbinu, S. K. (2021). Chemical thermodynamics determination of corrosion threshold assessment of reinforced concrete structures. *Saudi Journal of Engineering and Technology*, *6*(8), 242-258. https://doi.org/10.36348/sjet.2021.v06i08.004
- Al-Moudi, O. S. B., Maslehuddin, M., Lashari, A. N., & Almusallam, A. A. (2003). Effectiveness of corrosion inhibitors. *Cement and Concrete Composites*, *25*(4), 439-449. https://doi.org/10.1016/S0958-9465(02)00086-0
- Charles, K., Irimiagha, P. G., & Bright, A. (2018). Investigation of corrosion potential probability and concrete resistivity of inhibited reinforcement chloride threshold in corrosive environment. *International Journal of Scientific & Engineering Research*, *9*(4), 1696-1713.
- Charles, K., Nwinuka, B., & Philip, K.F.O. (2018). Investigation of corrosion probability assessment and concrete resistivity of steel inhibited reinforcement of reinforced concrete structures on severe condition. *International Journal of Scientific & Engineering Research*, *9*(4), 1714-1730.
- Dalo-Abu, A. M., Othman, A. A., & Rawashdeh, A. I. (2012). Exudate gum from Acacia trees as green corrosion inhibitor for mild steel in acidic media. *International Journal of Electrochemical Science, 7*, 9303-9324.
- Gaidis, J. M., & Rosenberg, A. M. (1987). The inhibition of chloride-induced corrosion in reinforced concrete by calcium nitrite. *Cement, Concrete and Aggregates*, *9*(1), 30-33. https://doi.org/10.1520/CCA10143J
- Gowers, K. R., & Millard, S. G. (1999a). Electrochemical techniques for corrosion assessment of reinforced concrete structures. *Institution of Civil Engineers - Structures and Buildings*, *134*(2), 129-137. https://doi.org/10.1680/istbu.1999.31475
- Gowers, K. R., & Millard, S. G. (1999b). Measurement of concrete resistivity for assessment of corrosion severity of steel using Wenner technique. *ACI Materials Journal*, *96*(5), 536-541. https://doi.org/10.14359/646

- Hansson, C. M., Mammoliti, L., & Hope, B. B. (1998). Corrosion inhibitors in concrete – Part I: The principles. *Cement and Concrete Research, 28*(12), 1775-1781. https://doi.org/10.1016/S0008-8846(98)00168-3
- Jano, A., Lame, A., & Kokalari, E. (2012). Use of extracted green inhibitors as a friendly choice in corrosion protection of low alloy carbon steel. *Kemija u Industriji, 61*(11-12), 497-503. https://doi.org/10.15255/KUI.2011.012
- Joiret, S., Keddam, M., Nóvoa, X. R., Pérez, M. C., Rangel, C., & Takenouti, H. (2002). Use of EIS, ring-disk electrode, EQCM and Raman spectroscopy to study the film of oxides formed on iron in 1 M NaOH. *Cement and Concrete Composites, 24*(1), 7-15. https://doi.org/10.1016/S0958-9465(01)00022-1
- Justnes, H. (2003). Inhibiting chloride induced corrosion of concrete bars by calcium nitrite addition. Corrosion, Paper No. 03287. https://doi.org/10.5006/1.3277580
- Layssi, H., Ghods, P., Alizadeh, A. R., & Salehi, M. (2015). Electrical resistivity of concrete: Concepts, applications, and measurement techniques. *Concrete International, 37*(1), 41-46.
- Luo, D., Li, Y., Lim, K. S., & Mohd Nazal, N. A. (2018). A recent progress of steel bar corrosion diagnostic techniques in RC structures - A review. *Sensors, 19*(1), 19-34. https://doi.org/10.3390/s19010034
- Macmammah, M., Gbinu, S. K., & Charles, K. (2021). Chloride threshold ingress evaluation of corrosion probability using concrete electrical resistivity and half-cell potential measurements. *Scholars International Journal of Chemistry and Material Science, 4*(7), 204-220. https://doi.org/10.36348/sijcms.2021.v04i07.004
- Ormellese, M., Berra, M., Bolzoni, F., & Pastore, T. (2006). Corrosion inhibitors for chlorides-induced corrosion in reinforced concrete structures. *Cement and Concrete Research, 36*(3), 536-547. https://doi.org/10.1016/j.cemconres.2005.12.014
- Poursaee, A., & Hansson, C.M. (2007). Reinforcing steel passivation in mortar and pore solution. *Cement and Concrete Research, 37*(7), 1127-1133. https://doi.org/10.1016/j.cemconres.2007.04.005
- Soylev, T. A., & Richardson, M. G. (2008). Corrosion inhibitors for steel in concrete: State-of-the-art report. *Construction and Building Materials, 22*(4), 609-622. https://doi.org/10.1016/j.conbuildmat.2006.10.012
- Umoren, S. A. (2009). Synergistic influence of gum arabic and iodide ion on the corrosion inhibition of aluminum in alkaline medium. *Portugaliae Electrochimica Acta, 27*(5), 565-577. https://doi.org/10.4152/pea.20090565
- Umoren, S. A., Ogbobe, O., Igwe, I. E., & Ebenso, E. E. (2008). Inhibition of mild steel corrosion in acidic medium using synthetic and naturally occurring polymers and synergistic halide additives. *Corrosion Science, 50*(7), 1998-2006. https://doi.org/10.1016/j.corsci.2008.04.026
- Wang, K., & Monteiro, P. J. M. (1996). Corrosion products of reinforcing steel and their effects on the deterioration of concrete. Third CANMET/ACI International Conference on Durability of Concrete, SP170-37. 83-97.